第38卷第6期 2022年6月
无 机 化 学 学 报 CHINESE JOURNAL OF INORGANIC CHEMISTRY
Vol.38 No.6 1121-1132

基于金属离子交换的有机金属凝胶用于检测抗生素与硝基芳香族化合物

袁仪祯 杨云裳* 赵玉琛 张应鹏*
(兰州理工大学石油化工学院,兰州 730050)

摘要: 废水中有机化合物的快速检测一直是一个重要的问题。采用离子交换法制备了具有荧光特性的铽基金属有机凝胶MOG(Tb)。研究表明,即使存在其他有机化合物,微量的呋喃唑酮(FZD)、甲硝唑(MDZ)、2,4-二硝基甲苯(2,4-DNT)和4-硝基苯酚(4-NP)也能有效猝灭MOG(Tb)的荧光发射,证明MOG(Tb)干凝胶作为一种化学传感器可以有效检测抗生素(FZD、MDZ)和硝基芳香族化合物(2,4-DNT、4-NP)。有趣的是,青霉素钾(PCLP)却能增强MOG(Tb)的荧光。此外,还进行了MOG(Tb)干凝胶的可回收性和水稳定性试验,并得到了较为满意的结果。

关键词: 金属有机凝胶; 抗生素; 硝基芳香族化合物; 荧光猝灭
中图分类号: O614.341 **文献标识码:** A **文章编号:** 1001-4861(2022)06-1121-12
DOI: 10.11862/CJIC.2022.126

Organometallic Gels Based on Metal Ion Exchange for the Detection of Antibiotics and Nitroaromatic Compounds

YUAN Yi-Zhen YANG Yun-Shang* ZHAO Yu-Chen ZHANG Ying-Peng*
(*School of Petrochemical Engineering, Lanzhou University of Technology, Lanzhou* 730050, *China*)

Abstract: Rapid detection of organic compounds in wastewater has always been an important issue. Fluorescent Tb-based metal-organic gel MOG(Tb) was prepared by the metal ion exchange method. The studies have shown that trace amounts of furazolidone (FZD), metronidazole (MDZ), 2,4-dinitrotoluene (2,4-DNT), and 4-nitrophenol (4-NP) could effectively quench the fluorescence emission of MOG(Tb) even in the presence of other analytes, demonstrating that the MOG(Tb) xerogels could effectively detect antibiotics (FZD, MDZ) and nitroaromatic compounds (2,4-DNT, 4-NP). However, penicillin G potassium salt (PCLP) could enhance the fluorescence of MOG(Tb). In addition, the recyclability and water stability tests of the MOG(Tb) xerogels were also carried out, and satisfactory results were obtained.

Keywords: metal-organic gel; antibiotics; nitroaromatic compounds; fluorescence quenching

0 Introduction

Since the introduction of penicillin in 1929, antibiotics have been a great boon to improving human and animal health[1-2]. In some countries, veterinary antibiotics are also frequently added to animal feeds to improve growth rates and feed efficiency[3-5]. However, most antibiotics tested to date are not biodegradable under aerobic conditions[6-7]. The adverse effects of antibiotics on higher aquatic organisms have been reported[8-9]. In aquaculture, widely used antimicrobials can cause skeletal deformation[10]. Antimicrobials may have qualitative and quantitative effects on resident microbial communities found in sediments[11-12], thereby affect-

收稿日期:2021-12-02。收修改稿日期:2022-03-30。
*通信联系人。E-mail:yingpengzhang@126.com,yangyunshang@tom.com

ing the degradation of organic matter[13]. Nitroaromatics are also among the organic pollutants and antibiotics found in wastewater[14]. At the same time, the rapid detection of explosives (such as nitroaromatic compounds) and explosives-like is also a very important aspect related to homeland security[15-17] and environmental safety[18].

There are many methods to detect antibiotics and organic explosives, including electrochemical methods[20], infrared spectroscopy[19], and liquid chromatography[21]. However, these methods are limited by complex operations and costs[22]. Therefore, there is an urgent need to explore a simple and effective strategy for antibiotic detection[23]. Fluorescence quenching-based detection methods[24-25] are a very promising method[28] with the advantages of high efficiency[26], low cost[27], and short reaction time.

Although metal-organic frameworks (MOFs) are often used to detect a variety of substances[29], metal-organic gels (MOGs) are very rare as a new type of material[30]. Compared to MOFs, MOGs have a smaller density, lower crystallinity, and larger surface area[31-34], which would be very beneficial for the detection of antibiotics and nitroaromatic compounds (NACs) [35-36]. However, the development of MOGs has only just begun and much work[38] remains to be done on MOGs due to uncertainties such as their gelation process and structure[37].

In this work, inspired by the metal replacement method, Al-based MOG (MOG(Al)) achieved irreversible partial metal ion exchange. With this post-treatment, the Al ion-based gel was converted into a metal-organic gel containing rare-earth ions (MOG(Tb)). Unexpectedly, due to its intense fluorescence and excellent water stability, it showed high selectivity and sensitive detection of antibiotics and NACs. Moreover, the method here is very convenient and feasible for the large-scale synthesis of MOG agglomerates. This will open up a new avenue for the application of MOG materials.

1 Experimental

1.1 Materials and general methods

According to the reference[39], 4,4,4-tricarboxylic acid triphenylamine (H_3TCA) was synthesized by Friedel-Crafts acylation reaction (Scheme 1). All other chemical reagents were directly purchased through merchants, and the purity was sufficient, no further processing was required. The powder X-ray diffraction (PXRD) pattern was gained on a Rigaku Ultima Ⅳ polycrystalline powder X-ray diffractometer, where the radiation source was Cu $K\alpha$ target, λ=0.154 06 nm, U=40 kV, I=30 mA, scanning range 2θ=5°-90°, scanning speed was 5 (°)·min^{-1}. The UV-Vis spectrophotometer model was UV-2700, from Varin, USA. The fluorescence spectrophotometer was F-7000 from Varin, USA. The thermogravimetric (TG) curve was recorded in a Q5000IR thermal analyzer, and the heating rate was 10 ℃·min^{-1} in nitrogen. The nitrogen adsorption-desorption was carried out in Mike ASAP2020 HD.

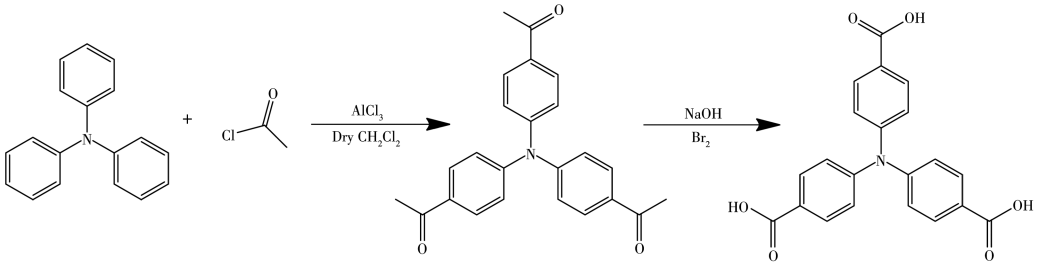

Scheme 1 Synthetic route of H_3TCA

1.2 Synthesis of MOG(Tb)

MOG(Al) was prepared by hydrothermal synthesis. $Al(NO_3)_3·9H_2O$ (0.375 1 g, 1 mmol) and H_3TCA (0.565 5 g, 1.5 mmol) were put into 20 mL ethanol and stirred well, then the solution was transferred to a steel autoclave lined with tetrafluoroethylene, heated at 140 ℃ for 8 h. After cooling to room temperature, the ocher gel was obtained, which was washed three times with ethanol. For the synthesis of homogeneous MOG(Al) gel, the molar ratio between the metal source and the

ligand was 2∶3.

The xerogel of MOG(Al) was soaked in an ethanol solution containing $Tb(NO_3)_3 \cdot 6H_2O$ (30 mL, 3 mmol) for 4 d to obtain MOG(Tb). After soaking, the gel was washed with ethanol to remove excess Tb^{3+} ions, centrifuged to remove the supernatant, and then dried at 70 ℃ for 12 h to obtain a xerogel of MOG(Tb).

1.3 Water stability test

To test the stability of MOG(Tb) in water, the powder sample of the xerogel was soaked in water with different pH values (2, 3, 5, 7, 9, 11, and 12) for 48 h, after drying all samples were tested by PXRD.

1.4 Fluorescence experiment

The ultraviolet absorption spectrum of MOG(Tb) was measured, then the solution was diluted so that the absorbance was between 0.06 and 0.08. The excitation wavelength was 355 nm, and the slit width was 8.5 nm for excitation and emission. The absorbance at the fluorescence emission wavelength and the absorption maximum wavelength in a range of 355-540 nm were measured.

Using the fluorescence quantum yield of quinine sulfate in 0.1 $mol \cdot L^{-1}$ sulfuric acid solution as the benchmark (Φ_r=0.58), the fluorescence quantum yields of MOG(Al) and MOG(Tb) were calculated by the following formula:

$$\Phi_r = \frac{n_r^2}{n_g^2} \times \frac{A_r \times I_g}{A_g \times I_r} \times \Phi_r$$

where n is the refractive index of the solution, A is the absorbance of the compound at the excitation wavelength, r represents the reference compound, I is the fluorescence intensity of the compound, g represents the gel compound sample, and Φ is the fluorescence quantum yield of the sample.

To effectively detect antibiotics and NACs, 4 mg of the MOG(Tb) xerogel powder was put into a 15 mL aqueous solution of antibiotics and organic explosives (c=0.4 $mmol \cdot L^{-1}$) at room temperature. All the mixtures were sonicated for 50 min to become stable suspensions.

Selective detection was then performed: (1) 4 mg of MOG(Tb) xerogel powder was added to furazolidone (FZD) and metronidazole (MDZ) aqueous solutions (0.4 $mmol \cdot L^{-1}$), respectively, and other antibiotics were added; (2) 4 mg of MOG(Tb) xerogel powder was put into an aqueous solution (0.4 $mmol \cdot L^{-1}$) of 2, 4-dinitrotoluene (2,4-DNT) and 4-nitrophenol (4-NP), and other NACs were added. All the mixtures were also sonicated for 40 min.

1.5 Cytotoxicity test

To examine the biocompatibility of MOG(Tb), the MTS (3-(4,5-dimethylthiazol-2-yl)-5-(3-carboxymethoxyphenyl)-2-(4-sulopheny)-2*H*-tetraolium, inner salt) method was used to detect the toxicity of MOG(Tb) to pig kidney cells (PK cells) and baby hamster Syrian kidney cells (BHK cells). First, PK and BHK cells were cultured using Dulbecco′s modified Eagle medium (DMEM) containing 10% fetal bovine serum (FBS) in a humid air environment with a temperature of 37 ℃ and a 5% volume fraction of CO_2. Then DMEM was used to prepare the dried sample into a homogeneous solution, and the solutions with concentrations of 10, 20, 100, 150, 200 $\mu g \cdot mL^{-1}$ were added to the cells, making six copies, and leaving a set of blanks as a comparison. After the cells were incubated for 24 h, 10 μL of MTS solution was added to the cells and incubated for 3 h. A microplate spectrophotometer was used to measure the optical density (OD) value of each well at a wavelength of 490 nm.

2 Results and discussion

2.1 Characterization of MOG(Al) and MOG(Tb)

Compared with conventional MOFs, MOGs have lower crystallinity and only a few broad peaks as seen by observation of PXRD. Similar characterization results have also been reported for xerogels. After metal ion exchange, the PXRD pattern of MOG(Tb) was almost identical to that of MOG(Al) (Fig.1a). Nitrogen adsorption-desorption tests were then performed to observe the porosity of MOG(Tb). As shown in Fig.1b, it was a Ⅰ-type isotherm, which was similar to the Langmuir-type adsorption isotherm, reflecting the micropore filling phenomenon, and indicating that MOG(Tb) has a certain microporous structure, and the saturated adsorption value is equal to the micropore. By NLDFT (nonlocal density functional theory) analy-

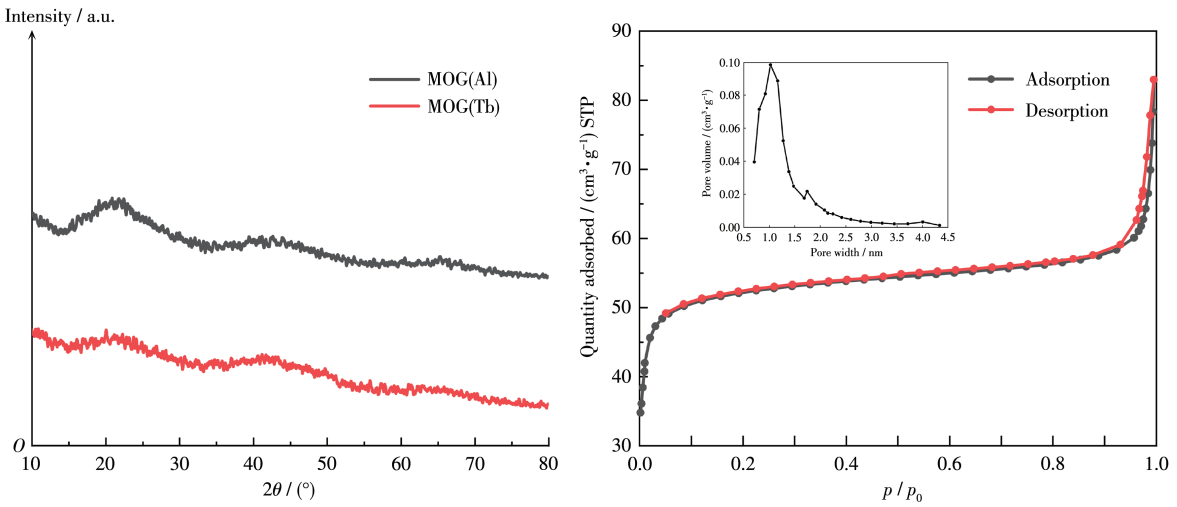

Inset: pore size distribution of MOG(Tb)

Fig.1 (a) PXRD patterns of MOG(Al) and MOG(Tb); (b) N_2 adsorption-desorption isotherms of MOG(Tb)

sis of nitrogen adsorption - desorption isotherms, the pore size distribution of MOG(Tb) was about 1.1 nm, and the BET (Brunauer - Emmett - Teller) specific surface area was about 168 $m^2 \cdot g^{-1}$.

As can be seen from the TG curves (Fig.S1, Supporting information), MOG(Al) and MOG(Tb) have similar thermal stability. There were two stages of weight loss from room temperature to 700 ℃ for MOG(Al). The first weight loss from room temperature to 300 ℃ is probably due to the solvent removal, removal of structural water, and volatilization of small molecular components. The subsequent weight loss can be attributed to the thermal effects of organic ligand decomposition and burning of the functional group. For MOG(Tb), the weight of the sample slowly decreased with increasing temperature. The weight of the sample decreased rapidly until 400 ℃. After the unstable groups in the sample have been decomposed, the weight of the sample did not change when the temperature was above 700 ℃, indicating that the organic components of the sample are completely oxidized to carbon dioxide and other relatively stable small molecular gaseous products. The difference in thermal stability of the two MOG compounds may be due to the fact that MOG(Al) is formed at high temperatures, whereas MOG(Tb) only undergoes ion exchange at room temperature, although the central ion has a larger radius and can be accommodated at the periphery. The more ligands there are, the larger the ionic radius of Tb and the less attractive it is to the ligand, which in turn will be the case and the coordination number will decrease.

The substitution effect of the metal ions Al^{3+} and Tb^{3+} was verified by ICP - OES (inductively coupled plasma - optical emission spectroscopy) tests. Table S1 summarizes the ion concentrations of Al^{3+} and Tb^{3+} in the xerogels before and after 3, 7, and 15 d of replacement. The concentration of Al^{3+} decreased as the replacement period increased, while the concentration of Tb^{3+} gradually increased, reaching a peak at 7 d of replacement. The results indicate that the ions in the gels have been successfully exchanged. The substitution of Al^{3+} may be due to the stronger interaction between the Tb^{3+} and the main group of the polycarboxylic acid.

2.2 Fluorescence characteristics, stability, and cytotoxicity of MOG(Tb)

After ion exchange, we can see that the product has obvious Tb^{3+} characteristic emission (Fig. 2). The obvious characteristic peak of MOG(Tb) at 418 nm is due to the $^5D_3 \rightarrow {}^7F_5$ transition of Tb^{3+}. The characteristic peak at 538 nm can be attributed to the $^5D_4 \rightarrow {}^7F_5$ transition. Compared with the weak fluorescence emission of H_3TCA at 425 nm, due to the charge transfer between the ligand and the metal, the coordination between Tb^{3+} and H_3TCA makes the xerogel have stronger fluorescence at 418 and 538 nm (Fig.S2). The fluo-

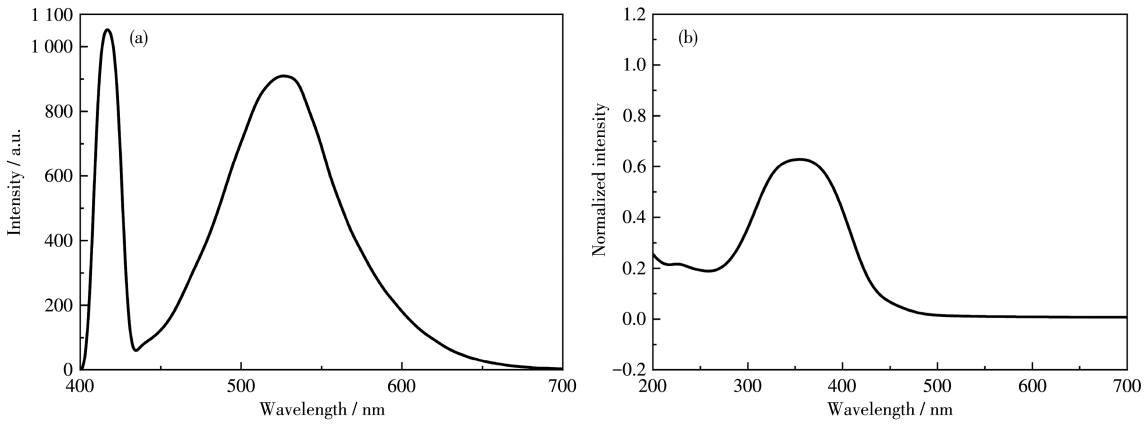

Fig.2　(a) Emission and (b) excitation spectra of MOG(Tb)

rescence quantum yields were calculated, and $\Phi_{MOG(Al)}$= 0.261, $\Phi_{MOG(Tb)}$=0.273. It can be seen that Tb^{3+} as the central ion has a better luminescence effect than Al^{3+}, and the energy transfer efficiency with the ligand is also higher.

In addition, the framework and structure of MOG(Tb) remained intact after soaking in pH=2, 3, 5, 7, 9, 11, and 12 for 48 h (Fig. 3), and it can be seen from Fig. S3 that the N_2 adsorption-desorption isotherms did not change significantly after the xerogel was immersed in the aqueous solutions with pH=2 and 12. To further examine the stability of the structure, MOG(Tb) was sonicated in aqueous solutions with different pH values, and then Al^{3+} and Tb^{3+} in the aqueous solutions were detected by titration and chromogenic methods, respectively. NaOH solution was added dropwise to the aqueous solutions with pH=2, 3, 5, 7, 9, 11, and 12 after ultrasonic treatment. It can be seen that

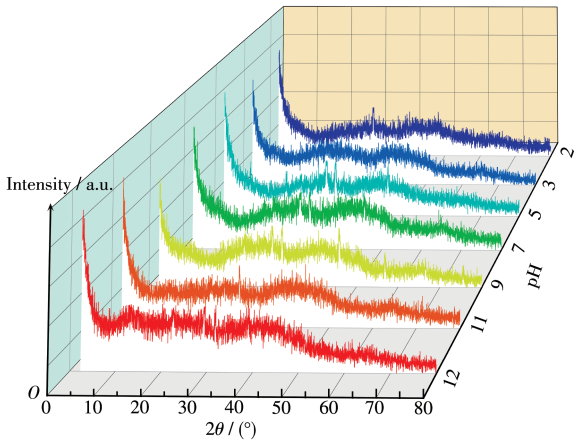

Fig.3　PXRD patterns of MOG(Tb) in aqueous solutions with pH=2, 3, 5, 7, 9, 11, and 12

there was a small amount of white precipitate in the aqueous solution with pH=2 and 12, but there was no precipitation in other solutions (Fig. S4). It can be concluded that a small amount of Al^{3+} was released into the aqueous solution with pH=2 and 12. Then, ammonium oxalate was used to detect the free Tb^{3+} content in aqueous solutions with different pH values after ultrasonication. 0.05 mL of the aqueous solution was pipetted with a micropipette and placed on filter paper. After drying with hot air, saturated ammonium oxalate solution was sprayed. If there are Tb ions, it will show yellow-green fluorescence under ultraviolet light. We can see that at pH=2, a few Tb^{3+} ions were released in an aqueous solution (Fig. S5).

As shown in Fig. S6, after 24 h of incubation, the survival rate of PK cells was still greater than 76%, and the survival rate of BHK cells was greater than 83%. These results indicate that MOG(Tb) has relatively low cytotoxicity.

2.3　Detection of antibiotics and NACs

Due to the superior water stability and excellent fluorescence emission of the xerogel, we were able to use MOG(Tb) to detect some antibiotics. We used nine antibiotics for the assay, namely sulfamethazine (SMZ), sulfadiazine (SDZ), FZD, MDZ, dimetridazole (DTZ), ornidazole (ODZ), chloramphenicol (CAP), florfenicol (FFC), and penicillin G potassium salt (PCLP). As can be seen in Fig. 4, MDZ and FZD had the highest quenching efficiencies of 91.2% and 94.7%, respectively. Interestingly, PCLP enhanced the fluorescence of MOG(Tb). The quenching efficiencies of DTZ and

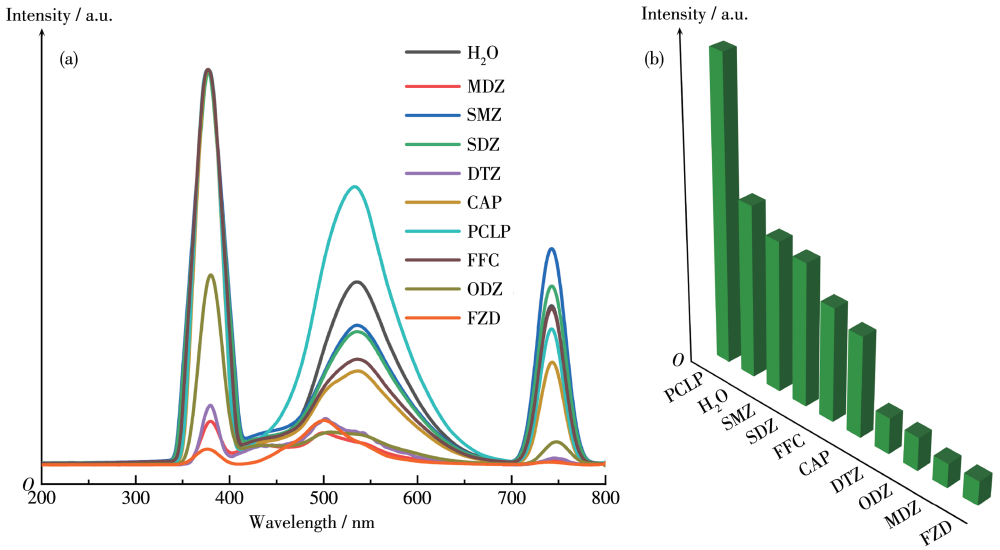

Fig.4 (a) Emission spectra and (b) fluorescence intensity at 538 nm of MOG(Tb) in various antibiotic aqueous solutions

ODZ were average. The quenching efficiencies of the other types of antibiotics were weaker. To quenching intensity of these antibiotics were ranked in the order of FZD > MDZ > ODZ > DTZ > CAP > FFC > SDZ > SMZ > PCLP. PXRD testing of the antibiotic-tested MOG(Tb) xerogel powder in turn showed that the structure and skeleton of the xerogel remained unchanged significantly (Fig.S4). Compared to Fig.2a, the leftward shift of the peak near 420 nm in Fig.4a may be due to the up-conversion process. When MOG(Tb) is mixed with the antibiotic solution, the luminescent center can absorb more photon energy and then produce emitted photons of higher energy than each excited photon. The absorption process for each photon is a binary primitive reaction due to the presence of an excited intermediate state. The "new peak" at 740 nm was the emission spectrum, which is due to the transition of electrons to different excited-state energy levels, absorbing different wavelengths of energy and producing different absorption bands, resulting in fluorescence of a certain wavelength.

To more clearly explain the fluorescence quenching effect of MOG(Tb) on MDZ and FZD, we tested the change of xerogel's fluorescence intensity as the antibiotic concentration gradually increased where each concentration gradient was increased by adding a 2 μL antibiotic solution (Fig. 5a and 5c). The quenching effect can be rationally calculated using the Stern-Volmer (SV) equation: $I_0/I=1+K_{SV}c_Q$, where I_0 and I are the fluorescence intensity of MOG(Tb) without adding and adding a certain concentration of the antibiotic solution, respectively, c_Q is the concentration of the antibiotic aqueous solution, and K_{SV} is the quenching constant. K_{SV} can be obtained by plotting $1/(I_0-I)$ against $1/c_Q$ and performing a linear fit.

For MOG(Tb), the quenching constants of FZD and MDZ were 7.76×10^4 and 8.03×10^4 L·mol^{-1}, respectively (Fig.5b and 5d). The values of the limit of detection (LOD=$3\sigma/K_{SV}$) for FZD and MDZ were 0.668 and 1.27 μmol·L^{-1} (Table S2). The quenching constant of FZD and MDZ to MOG(Tb) was also higher than some reported MOF materials (Table 1), which is sufficient to prove its excellent quenching ability.

The selective detection ability of the xerogel for antibiotics is also very important in practical applications. To demonstrate the selective detection of FZD and MDZ by MOG(Tb), we performed control experiments. First, the fluorescence intensity of MOG(Tb) dispersed in water was tested, and then other antibiotics (30 μL) and the corresponding FZD and MDZ aqueous solutions (30 μL) were added to observe the change in fluorescence intensity. Fluorescence quenching occurred immediately after the addition of selected antibiotics FZD and MDZ to MOG(Tb) aqueous solutions containing other antibiotics, as shown in Fig. 6, with negligible effects of other antibiotics. The above

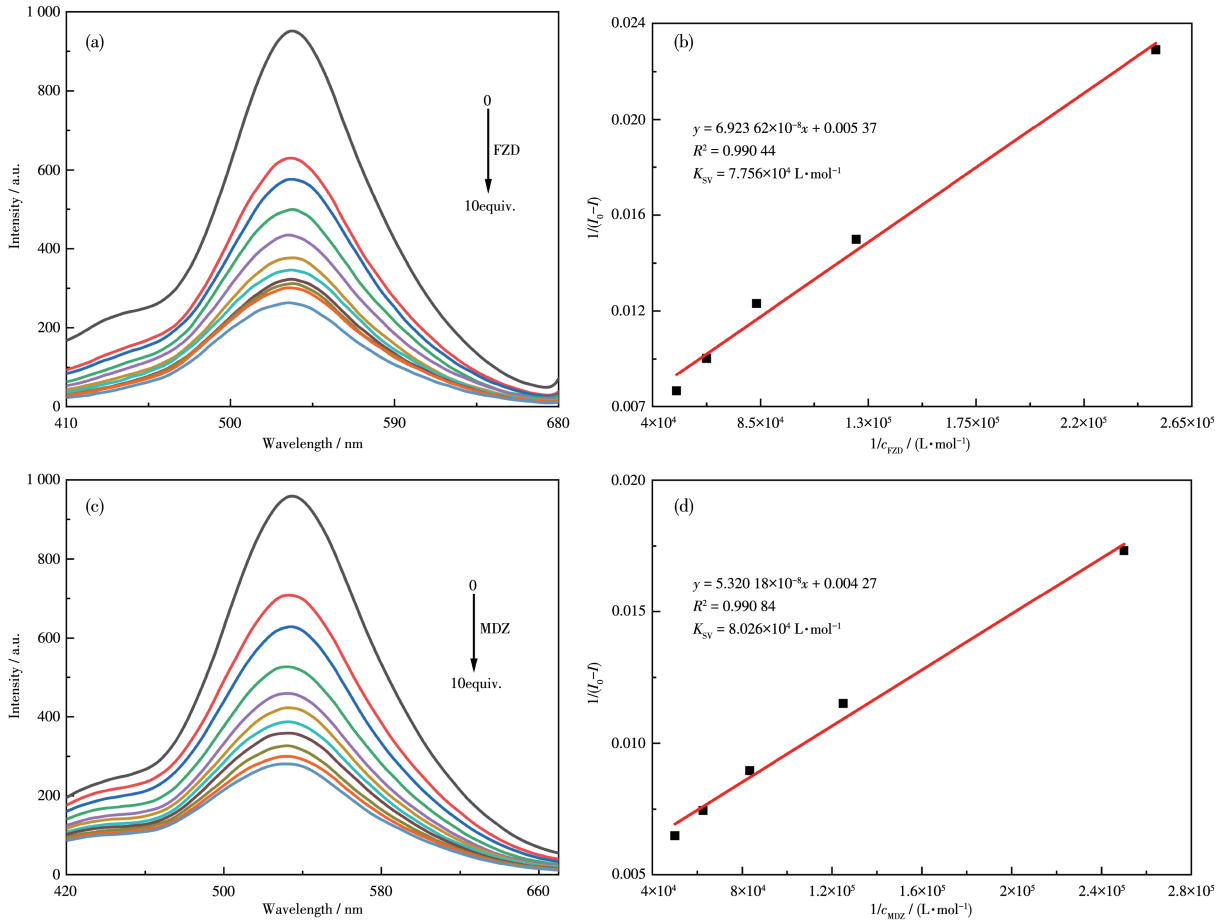

Fig.5　Emission spectra of MOG(Tb) with the gradually increasing (a) FZD and (c) MDZ concentrations; Linear fitting of SV equation for the fluorescence of MOG(Tb) quenched by (b) FZD and (d) MDZ in aqueous solution

Table 1　Summary of quecking constants (K_{SV}) of related materials for FZD, MDZ, 2,4-DNT, and 4-NP

Analyte	K_{SV} / (L·mol^{-1})	Reference
FZD	1.08×10^4	[40]
FZD	1.50×10^4	[41]
FZD	3.77×10^4	[42]
FZD	7.76×10^4	This work
MDZ	1.30×10^4	[43]
SMDZ	1.80×10^4	[44]
MDZ	1.10×10^4	[45]
MDZ	2.39×10^4	[46]
MDZ	8.03×10^4	This work
2,4-DNT	2.50×10^4	[43]
2,4-DNT	2.65×10^4	This work
4-NP	2.2×10^4	[47]
4-NP	8.58×10^4	This work

experiments demonstrate the high selectivity and sensitivity of MOG(Tb) for FZD and MDZ. Furthermore, we also found that the dropwise addition of PCLP solution to MOG(Tb) solution resulted in enhanced fluorescence (Fig. 4a). Although the specific fluorescence enhancement mechanism is unclear, we believe that the improved fluorescence properties can be attributed to the interaction of the carboxyl group of H_3TCA in MOG(Tb) with PCLP, resulting in the aggregation-induced emission (AIE) effect of the triphenylamine central structure.

Many researchers use unsaturated fatty acids for the detection of NACs, however, this method must be performed in organic solvents. It is more troublesome in practical application. Therefore, MOG(Tb) xerogels with excellent water stability and high-intensity fluorescence are particularly suitable for the detection of NACs. We selected 2, 4 - DNT, 2, 4, 6 - trinitrophenol (TNP), nitrobenzene (NB), 4 - NP, phenol (PHL), benzoic acid (BC), chlorobenzene (CB), toluene (MB), 2, 3 - dimethyl - 2, 3 - dinitrobutane (DMNB) to study their

effects on the fluorescence of MOG(Tb) in water. As shown in Fig.7, the quenching effect of 4-NP on the fluorescence of MOG(Tb) was the strongest, followed by 2,4-DNT. The quenching efficiencies of 2,4-DNT and 4-NP were 92.5% and 95.7%, respectively, while those of the other analytes were less than ideal. Their quenching efficiencies can be ordered as 4-NP > 2,4-DNT > NB > DMNB > MB > BC > TNP > CB > PHL. Moreover, after being immersed in an aqueous solution of antibiotics or small organic molecules for 24 h, the framework and structure of MOG(Tb) were still closely arranged with almost no change (Fig.S7 and S8).

Fluorescence quenching titration (Fig. 8a and 8c) and SV linear fitting (Fig. 8b and 8d) were performed for 2, 4 - DNT and 4 - NP, respectively. The K_{SV} for 2.4 - DNT and 4 - NP were 2.65×10^4 and 8.58×10^4 L·mol^{-1}, respectively, and the LOD values for 2, 4 - DNT and 4 - NP were 1.49 and 0.253 μmol·L^{-1}, respectively (Table S2). The K_{SV} values of MOG(Tb) for 2.4 - DNT and 4 - NP were higher or comparable to those of previously reported MOF materials, which demonstrates its good detecting ability (Table 1). In addition, we also analyzed and discussed the effect of other small organic molecules (TNP, DMNB, BC, MB, NB, CB, PHL) on the detection of 2,4-DNT and 4-NP by MOG(Tb). The fluorescence from MOG(Tb) was almost completely

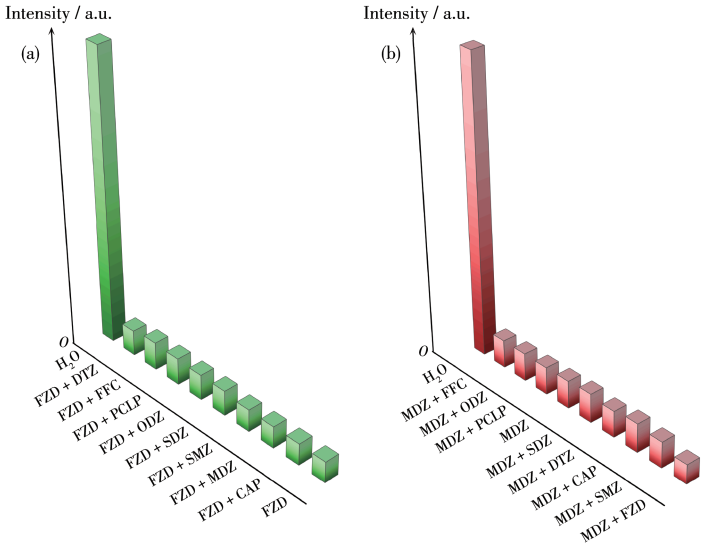

Fig.6 Fluorescence intensity of MOG(Tb) at 538 nm in the presence of (a) FZD/(b) MDZ and other antibiotics

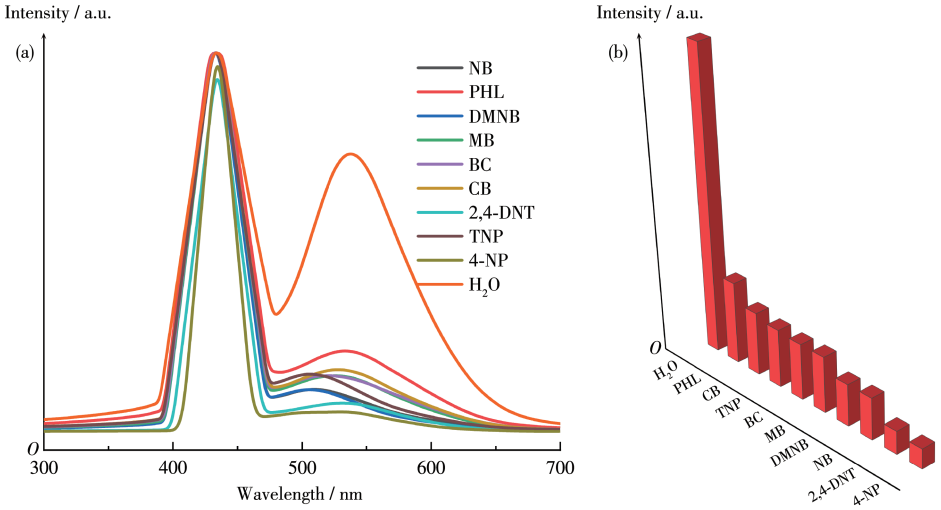

Fig.7 (a) Fluorescence spectra and (b) fluorescence intensity at 538 nm of MOG(Tb) in aqueous solutions of various small organic molecules

quenched when 2,4-DNT and 4-NP (30 μL) were added to an aqueous MOG(Tb) solution containing other analytes (Fig.9). Negligible effects of other small organic molecules on the analysis can be demonstrated, demonstrating the excellent selectivity and sensitivity of the xerogel for 2,4-DNT and 4-NP.

After detection, the xerogel could be washed with ethanol, filtered, and dried, and it still had a reproduc-

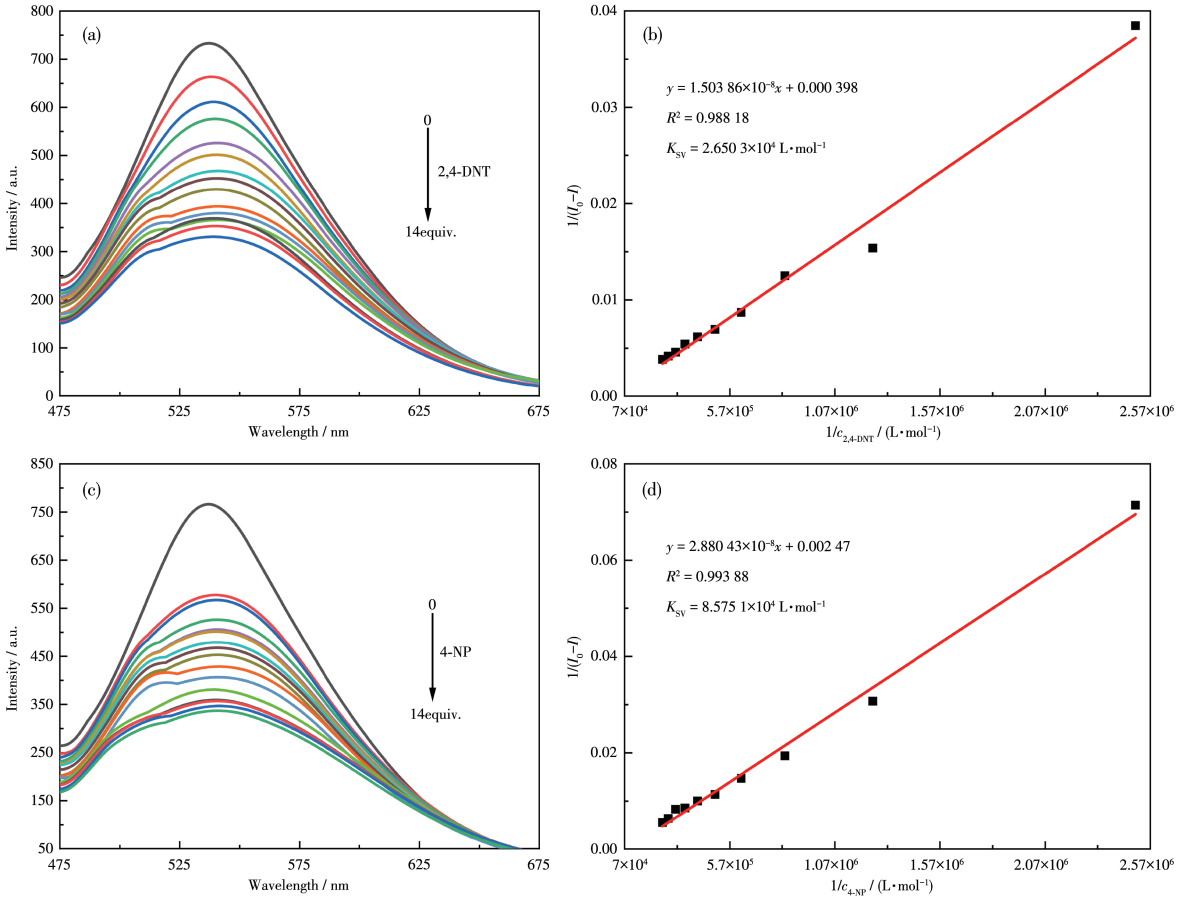

Fig.8　Emission spectra of the fluorescence quenching titration of MOG(Tb) by (a) 2,4-DNT and (c) 4-NP; SV linear fitting for the fluorescence of MOG(Tb) quenched by (b) 2,4-DNT and (d) 4-NP in aqueous solution

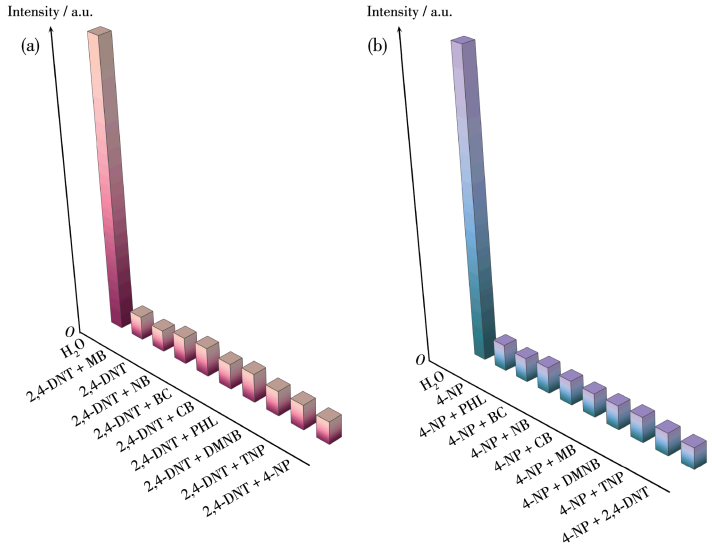

Fig.9　Fluorescence intensity of MOG(Tb) at 538 nm in the presence of (a) 2,4-DNT/(b) 4-NP and other small organic molecules

ible fluorescence quenching effect for detecting the analytes (Fig. 10). After 7 cycles of quenching experiments, the framework and structure of MOG(Tb) were still intact (Fig.S9). It could also be seen from the SEM image of MOG(Tb) that the structures were closely arranged (Fig. S10), proving that MOG(Tb) has good recyclability and stability.

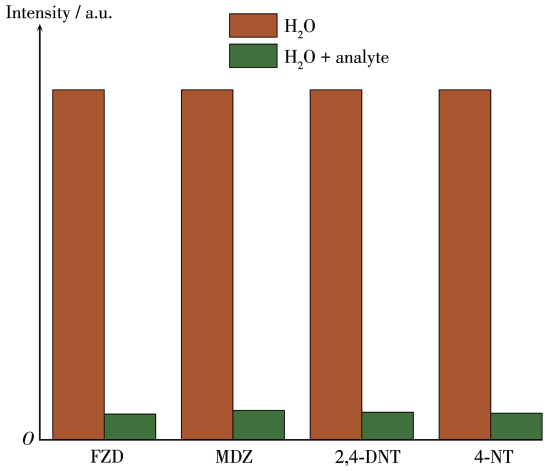

Fig.10 Reproducible fluorescence quenching effect for MOG(Tb) detecting the analytes

2.4 Mechanism of fluorescence quenching

We further explored the mechanism of fluorescence quenching MOG(Tb). UV-Vis spectra of the nine antibiotic analytes mentioned above and the nine NACs and non-NACs were examined (Fig. S11 and S12). It can be seen that the absorption bands of FZD and MDZ overlapped most of the excitation band of MOG(Tb) compared to the other antibiotic analytes, which may lead to lower absorption of the ligands of MOG(Tb). This implies that the stronger quenching of MOG(Tb) by FZD and MDZ is due to an energy transfer process between the ligands and metal ions[50]. For NACs and non-NACs, 2,4-DNT and 4-NP had the highest recombination and the mechanism can be inferred that the fluorescence quenching of MOG(Tb) by FZD, MDZ, 2,4-DNT, and 4-NP can be attributed to their competition with the ligands of MOG(Tb) [48]. FZD, MDZ, 2,4-DNT, and 4-NP absorb the excitation energy and reduce the ligand absorbed light, so the energy transfer from the ligand to the Tb^{3+} ion is reduced and the characteristic fluorescence of Tb^{3+} is subsequently quenched.

3 Conclusions

In summary, we prepared a gel named MOG(Al) based on the triphenylamine structure as the main ligand and then formed a xerogel named MOG(Tb) with strong fluorescence emission through metal ion exchange. And it has sensitive detectability for FZD, MDZ, 2,4-DNT, and 4-NP, and the detection limits are 0.668, 1.27, 1.49, 0.253 $\mu mol \cdot L^{-1}$ respectively. The quenching mechanism can be attributed to the interaction with the ligand competitive absorption. The preparation of MOG(Tb) can provide more possibilities for the development of MOG in the future.

Conflicts of interest: The authors declare no competing financial interest.

Supporting information is available at http://www.wjhxxb.cn

References:

[1]Alsaedi M K, Alothman G K, Alnajrani M N, Alsager O A, Alshmimri S A, Alharbi M A, Alawad M O, Alhadlaq S, Alharbi S. Antibiotic Adsorption by Metal-Organic Framework (UiO-66): A Comprehensive Kinetic, Thermodynamic, and Mechanistic Study. *Antibiotics*, **2020**,**9**(10):722

[2]Azhar M R, Abid H R, Sun H Q, Periasamy V, Tade M O, Wang S B. Excellent Performance of Copper Based Metal Organic Framework in Adsorptive Removal of Toxic Sulfonamide Antibiotics from Wastewater. *J. Colloid Interface Sci.*, **2016**,**478**:344-352

[3]Chai H M, Zhang G Q, Jiao C X, Ren Y X, Gao L J. A Multifunctional Tb-MOF Detector for H_2O_2, Fe^{3+}, $Cr_2O_7^{2-}$, and TPA Explosive Featuring Coexistence of Binuclear and Tetranuclear Clusters. *ACS Omega*, **2020**,**5**(51):33039-33046

[4]Cong Z Z, Song Z F, Ma Y X, Zhu M C, Zhang Y, Wu S Y, Gao E J. Highly Emissive Metal-Organic Frameworks for Sensitive and Selective Detection of Nitrofuran and Quinolone Antibiotics. *Chem. Asian J.*, **2021**,**16**(13):1773-1779

[5]Firuzabadi F D, Alavi M A, Zarekarizi F, Tehrani A A, Morsali A. A Pillared Metal-Organic Framework with Rich π-Electron Linkers as a Novel Fluorescence Probe for the Highly Selective and Sensitive Detection of Nitroaromatics. *Colloids Surf. A*, **2021**,**622**:126631

[6]Gai S, Zhang J, Fan R Q, Xing K, Chen W, Zhu K, Zheng X B, Wang P, Fang X K, Yang Y L. Highly Stable Zinc-Based Metal-Organic Frameworks and Corresponding Flexible Composites for Removal and Detection of Antibiotics in Water. *ACS Appl. Mater. Interfaces*, **2020**, **12**(7):8650-8662

[7]Gan Z Y, Hu X T, Xu X C, Zhang W, Zou X B, Shi J Y, Zheng K Y,

Arslan M. A Portable Test Strip Based on Fluorescent Europium-Based Metal-Organic Framework for Rapid and Visual Detection of Tetracycline in Food Samples. *Food Chem.*, **2021**,**354**:129501

[8]Guo F, Su C H, Fan Y H, Shi W B, Zhang X L. Construction of a Dual-Response Luminescent Metal-Organic Framework with Excellent Stability for Detecting Fe^{3+} and Antibiotic with High Selectivity and Sensitivity. *J. Solid State Chem.*, **2020**,**284**:121183

[9]Guo X, Gao B, Cui X, Wang J H, Dong W Y, Duan Q, Su Z M. PL Sensor for Sensitive and Selective Detection of 2, 4, 6-Trinitrophenol Based on Carbazole and Tetraphenylsilane Polymer. *Dyes Pigment.*, **2021**,**191**:109379

[10]Imanipoor J, Mohammadi M, Dinari M, Ehsani M R. Adsorption and Desorption of Amoxicillin Antibiotic from Water Matrices Using an Effective and Recyclable MIL-53(Al) Metal-Organic Framework Adsorbent. *J. Chem. Eng. Data*, **2021**,**66**(1):389-403

[11]Joseph L, Jun B M, Jang M, Park C M, Munoz-Senmache J C, Hernandez-Maldonado A J, Heyden A, Yu M, Yoon Y. Removal of Contaminants of Emerging Concern by Metal-Organic Framework Nanoadsorbents: A Review. *Chem. Eng. J.*, **2019**,**369**:928-946

[12]Li B, Jiang Y Y, Sun Y Y, Wang Y J, Han M L, Wu Y P, Ma L F, Li D S. The Highly Selective Detecting of Antibiotics and Support of Noble Metal Catalysts by a Multifunctional Eu-MOF. *Dalton Trans.*, **2020**,**49**(42):14854-14862

[13]Li C L, Zeng C H, Chen Z, Jiang Y F, Yao H, Yang Y Y, Wong W T. Luminescent Lanthanide Metal-Organic Framework Test Strip for Immediate Detection of Tetracycline Antibiotics in Water. *J. Hazard. Mater.*, **2020**,**384**:121498

[14]Li C P, Long W W, Lei Z, Guo L, Xie M J, Lu J, Zhu X D. Anionic Metal-Organic Framework as a Unique Turn-On Fluorescent Chemical Sensor for Ultra-Sensitive Detection of Antibiotics. *Chem. Commun.*, **2020**,**56**(82):12403-12406

[15]Li D, Lv N, Yu J K, Qiao Y, Xue X X, Li H J, Che G B. Synthesis, Crystal Structure and Highly Sensitive Detection Property of a Fluorescent Copper Coordination Polymer. *J. Mol. Struct.*, **2021**, **1236**: 130347

[16]Li J, Ye C F, Wu Y N, Zhu Y J, Xu J J, Wang Y, Wang H T, Guo M T, Li F T. Novel Sensing Platform Based on Gold Nanoparticle-Aptamer and Fe-Metal-Organic Framework for Multiple Antibiotic Detection and Signal Amplification. *Environ. Int.*, **2019**,**125**:135-141

[17]Li S Q, Liu X D, Chai H X, Huang Y M. Recent Advances in the Construction and Analytical Applications of Metal-Organic Frameworks-Based Nanozymes. *Trac-Trends Anal. Chem.*, **2018**,**105**:391-403

[18]Li W T, Hu Z J, Meng J, Zhang X, Gao W, Chen M L, Wang J H. Zn-Based Metal Organic Framework-Covalent Organic Framework Composites for Trace Lead Extraction and Fluorescence Detection of TNP. *J. Hazard. Mater.*, **2021**,**411**:125021

[19]Li Z P, Zhu X P, Gao E J, Wu S Y, Zhang Y, Zhu M C. Bifunctional Luminescent Eu Metal-Organic Framework for Sensing Nitroaromatic Pollutants and Fe^{3+} Ion with High Sensitivity and Selectivity. *Appl. Organomet. Chem.*, **2021**,**35**(3):e6136

[20]Liang X Q, Wen L X, Mi Y F, Guo J J, Yu B, Tao M, Cao Z H, Zhao Z J. Highly Cross-Linked Polymeric Nanoparticles with Aggregation-Induced Emission for Sensitive and Recyclable Explosive Detection. *Dyes Pigment.*, **2021**,**191**:109369

[21]Lin Z G, Song F Q, Wang H, Song X Q, Yu X X, Liu W S. The Construction of a Novel Luminescent Lanthanide Framework for the Selective Sensing of Cu^{2+} and 4-Nitrophenol in Water. *Dalton Trans.*, **2021**,**50**(5):1874-1886

[22]Liu S, Bai J L, Huo Y P, Ning B A, Peng Y, Li S, Han D P, Kang W J, Gao Z X. A Zirconium-Porphyrin MOF-Based Ratiometric Fluorescent Biosensor for Rapid and Ultrasensitive Detection of Chloramphenicol. *Biosens. Bioelectron.*, **2020**,**149**:111801

[23]Liu X G, Tao C L, Yu H Q, Chen B, Liu Z, Zhu G P, Zhao Z J, Shen L, Tang B Z. A New Luminescent Metal-Organic Framework Based on Dicarboxyl-Substituted Tetraphenylethene for Efficient Detection of Nitro-Containing Explosives and Antibiotics in Aqueous Media. *J. Mater. Chem. C*, **2018**,**6**(12):2983-2988

[24]Lu D K, Qin M H, Liu C, Deng J J, Shi G Y, Zhou T S. Ionic Liquid-Functionalized Magnetic Metal-Organic Framework Nanocomposites for Efficient Extraction and Sensitive Detection of Fluoroquinolone Antibiotics in Environmental Water. *ACS Appl. Mater. Interfaces*, **2021**,**13**(4):5357-5367

[25]Nacarogluballi J, Kirpik H, Kose M. A Gossypol-Hydrazone Compound and Its Sensing Properties towards Metal Ions and Nitro-Phenolic Compounds. *J. Mol. Struct.*, **2021**,**1236**:130310

[26]Qin Z S, Dong W W, Zhao J, Wu Y P, Tian Z F, Zhang Q, Li D S. Metathesis in Metal-Organic Gels (MOGs): A Facile Strategy to Construct Robust Fluorescent Ln-MOG Sensors for Antibiotics and Explosives. *Eur. J. Inorg. Chem.*, **2018**(2):186-193

[27]Qin Z S, Dong W W, Zhao J, Wu Y P, Zhang Q C, Li D S. A Water-Stable Tb(Ⅲ)-Based Metal-Organic Gel (MOG) for Detection of Antibiotics and Explosives. *Inorg. Chem. Front.*, **2018**,**5**(1):120-126

[28]Safaei M, Foroughi M M, Ebrahimpoor N, Jahani S, Omidi A, Khatami M. A Review on Metal-Organic Frameworks: Synthesis and Applications. *Trac-Trends Anal. Chem.*, **2019**,**118**:401-425

[29]Sharma V, Mehata M S. Rapid Optical Sensor for Recognition of Explosive 2, 4, 6-TNP Traces in Water through Fluorescent Znse Quantum Dots. *Spectrochim. Acta A*, **2021**,**260**:119937

[30]Singhaal R, Tashi L, Nisa Z, Ashashi N A, Sen C, Devi S, Sheikh H N. PEI Functionalized $NaCeF_4$: Tb^{3+}/Eu^{3+} for Photoluminescence Sensing of Heavy Metal Ions and Explosive Aromatic Nitro Compounds. *RSC Adv.*, **2021**,**11**(32):19333-19350

[31]Skorjanc T, Shetty D, Valant M. Covalent Organic Polymers and Frameworks for Fluorescence-Based Sensors. *ACS Sens.*, **2021**,**6**(4):1461-1481

[32]Sun S L, Sun X Y, Sun Q, Gao E Q, Zhang J L, Li W J. Europium Metal-Organic Framework Containing Helical Metal-Carboxylate Chains for Fluorescence Sensing of Nitrobenzene and Nitrofunans Antibiotics. *J. Solid State Chem.*, **2020**,**292**:121701

[33]Wang B, Lv X L, Feng D W, Xie L H, Zhang J, Li M, Xie Y B, Li J R, Zhou H C. Highly Stable Zr(Ⅳ)-Based Metal-Organic Frameworks

for the Detection and Removal of Antibiotics and Organic Explosives in Water. *J. Am. Chem. Soc.*, **2016**,**138**(19):6204-6216

[34]Wang G, Sun T T, Sun Z R, Hu X. Preparation of Copper Based Metal Organic Framework Materials and Its Effective Adsorptive Removal of Ceftazidime from Aqueous Solutions. *Appl. Surf. Sci.*, **2020**, **532**: 147411

[35]Wang B, Lv X L, Feng D, Xie L H, Zhang J, Li M, Zhou H C. Highly Stable Zr(Ⅳ)-Based Metal-Organic Frameworks for the Detection and Removal of Antibiotics and Organic Explosives in Water. *J. Am. Chem. Soc.*, **2016**,**138**(19):6204-6216

[36]Qin J H, Huang Y D, Shi M Y, Wang H R, Ma L F. Aqueous-Phase Detection of Antibiotics and Nitroaromatic Explosives by an Alkali-Resistant Zn-MOF Directed by an Ionic Liquid. *RSC Adv.*, **2020**,**10** (3):1439-1446

[37]Wang J, Zha Q Q, Qin G X, Ni Y H. A Novel Zn(Ⅱ)-Based Metal-Organic Framework as a High Selective and Sensitive Sensor for Fluorescent Detections of Aromatic Nitrophenols and Antibiotic Metronidazole. *Talanta*, **2020**,**211**:120742

[38]Wang K, Zhuang T, Su Z X, Chi M H, Wang H C. Antibiotic Residues in Wastewaters from Sewage Treatment Plants and Pharmaceutical Industries: Occurrence, Removal and Environmental Impacts. *Sci. Total Environ.*, **2021**,**788**:147811

[39]Wang J, He C, Wu P Y, Wang J, Duan C Y. An Amide-Containing Metal-Organic Tetrahedron Responding to a Spin-Trapping Reaction in a Fluorescent Enhancement Manner for Biological Imaging of NO in Living Cells. *J. Am. Chem. Soc.*, **2011**,**133**(32):12402-12405

[40]Xu Y L, Liu Y, Liu X H, Zhao Y, Wang P, Wang Z L, Sun W Y. Novel Cadmium(Ⅱ) Frameworks with Mixed Carboxylate and Imidazole-Containing Ligands for Selective Detection of Antibiotics. *Polyhedron*, **2018**,**154**:350-356

[41]Zhou S H, Lu L, Liu D, Wang J, Sakiyama H, Muddassir M, Liu J Q. Series of Highly Stable Cd(Ⅱ)-Based MOFs as Sensitive and Selective Sensors for Detection of Nitrofuran Antibiotic. *CrystEngComm*, **2021**,**23**(46):8043-8052

[42]Li J, Chen T J, Han S, Song L F. Four Zn(Ⅱ)-Organic Frameworks as Luminescent Probe for Highly Selectivity Detection of Cr(Ⅵ) Ions and Antibiotics. *J. Solid State Chem.*, **2019**,**277**:107-114

[43]Qin J H, Huang Y D, Shi M Y, Wang H R, Han M L, Yang X G, Ma L F. Aqueous-Phase Detection of Antibiotics and Nitroaromatic Explosives by an Alkali-Resistant Zn-MOF Directed by an Ionic Liquid. *RSC Adv.*, **2020**,**10**(3):1439-1446

[44]Wang G D, Li Y Z, Shi W J, Zhang B, Hou L, Wang Y Y. A Robust Cluster-Based Eu-MOF as Multi-functional Fluorescence Sensor for Detection of Antibiotics and Pesticides in Water. *Sens. Actuators B*, **2021**,**331**:129377

[45]Ji X X, Wu S Y, Song D X, Chen S Y, Chen Q, Gao E J, Xu J, Zhu X P, Zhu M C. A Water-Stable Luminescent Sensor Based on Cd^{2+} Coordination Polymer for Detecting Nitroimidazole Antibiotics in Water. *Appl. Organomet. Chem.*, **2021**,**35**(10):e6359

[46]Li J M, Li R, Li X. Construction of Metal-Organic Frameworks (MOFs) and Highly Luminescent Eu(Ⅲ)-MOF for the Detection of Inorganic Ions and Antibiotics in Aqueous Medium. *CrystEngComm*, **2018**,**20**(34):4962-4972

[47]Wang W, Yang J, Wang R M, Zhang L L, Yu J F, Sun D F. Luminescent Terbium-Organic Framework Exhibiting Selective Sensing of Nitroaromatic Compounds (NACs). *Cryst. Growth Des.*, **2015**, **15**(6): 2589-2592

[48]Abuzalat O, Wong D, Park S S, Kim S. Highly Selective and Sensitive Fluorescent Zeolitic Imidazole Frameworks Sensor for Nitroaromatic Explosive Detection. *Nanoscale*, **2020**,**12**(25):13523-13530

[49]Kaur M, Mehta S K, Kansal S K. A Fluorescent Probe Based on Nitrogen Doped Graphene Quantum Dots for Turn Off Sensing of Explosive and Detrimental Water Pollutant, TNP in Aqueous Medium. *Spectrochim. Acta A*, **2017**,**180**:37-43